

A Study of the Morphology of Polyurethane–Polystyrene Interpenetrating Polymer Networks by Means of Small Angle X-ray Scattering, Modulated-Temperature Differential Scanning Calorimetry, and Dynamic Mechanical Thermal Analysis Techniques

MO SONG, DOUGLAS J. HOURSTON, FRANZ U. SCHAFER

Institute of Polymer Technology and Materials Engineering, Loughborough University, Loughborough LE11 3TU, United Kingdom

Received 24 April 2000; accepted 7 June 2000

ABSTRACT: The morphology of polyurethane–polystyrene (PU-PS) (60 : 40 by weight) interpenetrating polymer networks (IPNs), in which internetwork grafting via 2-hydroxyethyl methacrylate residues (HEMA) (1, 2.5, and 10 wt %, respectively) in the polystyrene networks has been studied by means of small angle X-ray scattering (SAXS), modulated-temperature scanning calorimetry (M-TDSC), and dynamical mechanical thermal analysis (DMTA) techniques. With increasing internetwork grafting, the average size of domains became smaller (SAXS data) and the degree of component mixing increased (M-TDSC and DMTA results). For the PU-PS (60 : 40 by weight) IPN with 10% HEMA, the DMTA $\tan \delta$ -temperature plot showed a single peak. This DMTA result implied that the morphology of this PU-PS IPN is homogeneous. However, the M-TDSC data showed that three PU-PS (60 : 40) IPNs samples (with 1, 2.5, and 10 wt % HEMA, respectively) were phase separated. For the three IPN samples, the correlation length of the segregated phases, obtained from SAXS data based on the Debye–Bueche method, did not show distinct differences. With increasing internetwork grafting, the scattered intensity decreased. This study concluded that for these IPNs, SAXS is sensitive to the size of domains and component mixing, but no quantitative analysis was given for the component mixing. M-TDSC is suitable to be used to quantify the degree of component mixing or the weight fraction of interphases, and DMTA is sensitive to damping behavior and to phase continuity. However, DMTA cannot provide quantitative information about the degree of component mixing or the weight (or volume) fraction of the interphases. © 2001 John Wiley & Sons, Inc. *J Appl Polym Sci* 79: 1958–1964, 2001

Key words: interpenetrating polymer networks; small angle X-ray scattering; modulated-temperature differential scanning calorimetry

INTRODUCTION

Over the past twenty years, a substantial effort has gone into analyzing the detailed morphology of interpenetrating polymer networks (IPNs). The fundamental phenomenon associated with all IPNs is the phase separation occurring during IPN forma-

tion. The IPN properties are determined by phase continuity, domain size, interface content, and the degree of component mixing.

Transmission electron microscopy can be used to analyze IPN domain size and phase continuity.¹ Small angle X-ray scattering (SAXS) has been used to obtain information about interfaces^{2–4} in multiphase polymeric materials. Solid-state NMR spectroscopy has been used⁵ to estimate the degree of component mixing in IPNs based on the measurements of spin–lattice rela-

Correspondence to: M. Song (m.song@lboro.ac.uk).

Journal of Applied Polymer Science, Vol. 79, 1958–1964 (2001)
© 2001 John Wiley & Sons, Inc.

tion times. The results gave information about the intimacy of mixing of the two polymer networks. Winnik et al.⁶ studied the extent of component mixing in IPNs based on the analysis of direct nonradiative energy transfer measurements. They compared the results obtained from direct nonradiative energy transfer measurements with those of dynamic mechanical temperature analysis (DMTA) using the Fox equation.⁶ These analyses were based on a two-phase model. In some cases, it is difficult to describe the morphology of IPNs by a two-phase model, because the morphology of most of IPNs is multiphase.

Recent SAXS studies^{7,8} showed that it is difficult to obtain quantitative information about IPN interphases according to the analysis method suggested by Ruland.⁹ A different result¹⁰ from DMTA in which the $\tan \delta$ -temperature plot showed a single-peak for a polyurethane-poly(ethyl methacrylate) (70 : 30) IPN and from modulated-temperature differential scanning calorimetry (M-TDSC) in which the IPN showed a multiglass transition has been reported.

In this paper, three polyurethane (PU)-polystyrene (PS) (60 : 40 by weight) IPNs with 1, 2.5 and 10 wt % 2-hydroxyethyl methacrylate as internetwork grafting agent in PS component were prepared. Their morphologies were investigated by means of SAXS, M-TDSC, and DMTA. The aim in this paper is to compare the difference of information about the morphology of these IPNs provided by SAXS, M-TDSC, and DMTA, and to find out which technique can provide quantitative information about the degree of component mixing in IPNs.

EXPERIMENTAL

IPN Preparation

The preparation details for three PU-PS (60 : 40 by weight) IPN samples with 1, 2.5, and 10 wt % 2-hydroxyethyl methacrylate as internetwork grafting agent are as follows. The PU component comprised a tertiary diisocyanate, 1,1,3,3-tetramethylxylene diisocyanate (m-TMXDI) kindly donated by Cytec Industries), a polyoxypropylene glycol with a molar mass of 1025 (PPG1025) (BDH), and the crosslinker, trimethylol propane (TMP) (Aldrich). 2-Hydroxyethylmethacrylate (HEMA) (Aldrich) was used as a grafting agent. Stannous octoate (SnOC) (Sigma) was used as the PU catalyst. The other monomer used was styrene (S) (Aldrich).

The reaction was initiated with azoisobutyronitrile (AIBN) (Aldrich). The required amount of AIBN was dissolved in the monomer (S). In a separate receptacle, the triol (TMP) was dissolved in the PPG1025 at 60°C. Both components were combined at room temperature and the polyurethane catalyst was added. A nitrogen blanket was applied.

On addition of the TMXDL, the component was mixed for 5 min at high speed. Degassing for 1 min under vacuum was conducted to remove the entrapped air. The mixture was cast into stainless-steel spring-loaded O-ring molds, which had been pre-treated with CIL Release 1771 E release agent. The curing cycle consisted of three stages of 24 h each at 60, 80, and 90°C.

M-TDSC Measurements

A TA Instruments M-TDSC 2920 calorimeter was used. An oscillation amplitude of $\pm 1.0^\circ\text{C}$, an oscillation period of 60 s and a heating rate of $3^\circ\text{C}/\text{min}$ were used. The calorimeter was calibrated with a standard indium sample.

SAXS Measurements

SAXS measurements were undertaken on beamline 8.2 at the SRS, Daresbury Laboratory, Warrington, UK. The camera was equipped with a multiwire quadrant detector located approximately 1.0 m from the sample position. A vacuum chamber was placed between the sample and the detector in order to reduce air scattering and absorption. SAXS samples, approximately 0.5–0.9 mm thick, were prepared by casting. The scattering pattern from an oriented specimen of collagen was used to calibrate the SAXS detector. The experimental data were corrected for background scattering, sample thickness and transmission and the positional alinearity of the detector.

DMTA Measurements

Dynamic mechanical measurements were performed with a Polymer Laboratories MK II Dynamic Mechanical Analyser. Three samples were measured in the bending mode (single cantilever) at a fixed frequency of 10 Hz from -60 to 200°C using a heating ramp of $3^\circ\text{C}/\text{min}$. The test specimens were cut to a rectangular shape of about 50 mm in length, 10 mm in width, and 3 mm in thickness. The applied strain setting was $\times 4$.

RESULTS AND DISCUSSION

Figure 1 shows the scattered intensity versus scattering vector \mathbf{q} ($q = 4\pi/\lambda \sin \theta$; the λ is the

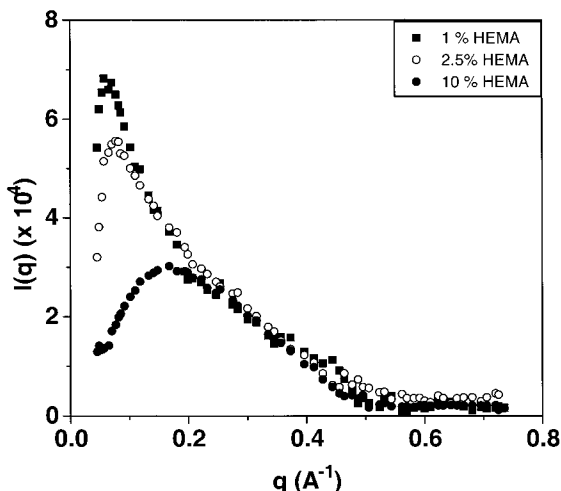


Figure 1 Scattered intensity versus q plots for the PU-PS (60 : 40 by weight) IPNs.

scattering wavelength (0.154 nm), and the θ is the scattering angle) for the three PS-PU IPNs. There is a distinct scattering peak in each SAXS plot. With increasing amount of the internetwork grafting agent in the PS component, the peak position shifted to higher scattering angles. This indicates that the size of the domains is becoming smaller with increasing amount of the internetwork grafting agent in the PS component. It has been reported^{11–13} that internetwork grafting can reduce phase separation and create smaller domains. The SAXS data confirmed this point. With increasing amount of the internetwork grafting agent in the PS component, the scattered intensity decreases which may result from the increase of the degree of component mixing in these IPNs.

SAXS by an ideal, two-phase system with sharp boundaries has been treated by Porod.¹⁴ The scattered intensity at large values of s ($s = 2/\lambda \sin \theta$) was found to be proportional to the reciprocal fourth power of s .

$$\lim_{S \rightarrow \infty} [I(s)] = K/s^4 \quad (1)$$

K is the Porod-law constant. This means that in the large-angle region, the product, $I(s)s^4$, becomes constant. However, in polymers, a deviation from the Porod law has been observed. Ruland⁹ has shown that the Porod law may be modified to include both positive deviations and negative deviations. The presence of thermal density fluctuations or mixing within phases results in an enhancement of scattering at high angles.

The deviations appear to be due to disorder, thermal motion, or the onset of wide-angle scattering.^{15–17} Thermal density fluctuations result in positive deviations from Porod's law. After considering this effect, the scattered intensity is given by

$$\lim_{S \rightarrow \infty} [I_{\text{obs}}(s)] = I(s)H^2(s) + I_b(s) \quad (2)$$

$I(s)$ is the Porod-law intensity and $H^2(s)$ is the Fourier transform of the autocorrelation smoothing function, which causes the negative deviations from Porod's law due to diffuse interphases. $I_b(s)$ is the scattering background due to electron-density fluctuations within the phases. According to Ruland, the scattered intensity at relatively high angles can be fitted empirically by

$$I_b(s) = I_0 \exp(bs^2) \quad (3)$$

The b is a constant and I_0 is the intensity value extrapolated to zero angle. If the intensities are absolute, the value of I_0 reflects the magnitude of the thermal density fluctuations. The three observed scattered intensities have been corrected for the background by subtracting the contribution of the thermal density fluctuations.

The diffuse phase boundary, on the other hand, causes a reduction of high-angle scattering resulting in a negative deviation. The electron-density profile $\Delta\rho_{\text{obs}}(r)$, may be represented as follows⁹:

$$\Delta\rho_{\text{obs}}(r) = \Delta\rho(r)h(r) \quad (4)$$

The r is the distance along an arbitrary vector inside the scattering volume. The $h(r)$ is a smoothing function, and $\Delta\rho(r)$ is the electron-density difference between the two phases.

The scattered intensity at a large value of s can be written⁹ as

$$\lim_{S \rightarrow \infty} [I_{\text{obs}}(s)] = I(s)H^2(s) \quad (5)$$

For the sigmodal-gradient model,^{9,17} the smoothing function is Gaussian.

$$H(s) = \exp(-2\pi^2\sigma^2s^2) \quad (6)$$

and the corresponding Porod law relation becomes

$$I_{\text{obs}}(s) = K/s^4 \exp(-4\pi^2\sigma^2s^2) \quad (7)$$

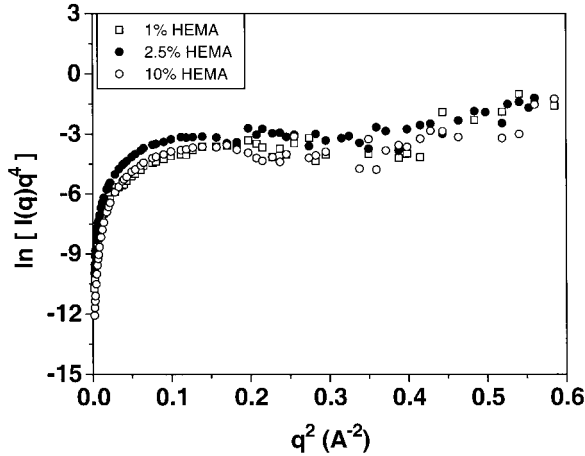


Figure 2 Plots of $\ln[I(q)q^4]$ versus q^2 for the PU-PS (60 : 40 by weight) IPNs.

Plots of $\ln[I(s)s^4]$ versus s^2 for the scattering data for the three PU-PS IPNs are shown in Figure 2. According to eq. (7), such plots will give negative slopes with diffuse domain boundaries, and the interphase thickness can be estimated from $[-(\text{slope})/4\pi^2]^{1/2}$. However, for the three PU-PS IPN samples, the plots all had positive slopes.

Applying the Debye–Bueche theory of X-ray scattering from isotropic but inhomogeneous systems,⁹ the intensity of a scattering system satisfies the scattering equation as follows:

$$I(s) = K\langle\eta^2\rangle \int_0^\infty \gamma(r)\{\sin(2\pi sr)/2\pi sr\}r^2 dr \quad (8)$$

K is a constant, η is the power fluctuation of the scattering system, which equals the difference between the electron density of the phases at the scattering angle, and γ is a correlation function.

The correlation function can be obtained by the Fourier transformation of the scattering intensity. For an undefined morphological structure, the correlation function can be given by the following empirical equation¹⁸:

$$\gamma(r) = \exp(-r/a_c) \quad (9)$$

The coefficient a_c , represents the correlation distance defined as the size of the heterogeneity in the system. Then, the scattered intensity can be obtained as follows:

$$I(s) = K\langle\eta^2\rangle a_c^3 (1 + 4\pi^2 s^2 a_c^2)^{-2} \quad (10)$$

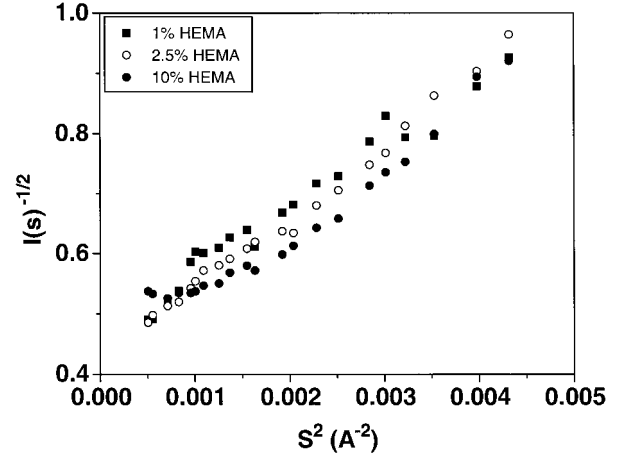


Figure 3 Plots of $I(s)^{-1/2}$ versus s^2 for the PU-PS (60 : 40 by weight) IPNs.

Therefore, plotting $I(s)^{-1/2}$ versus s^2 , the well-known Debye–Bueche plot, should produce a straight line with a slope-to-intercept ratio from which the correlation length a_c , can be obtained.

$$a_c = (\text{slope/intercept})^{1/2}/2\pi \quad (11)$$

Figure 3 shows the plots of $I(s)^{-1/2}$ versus s^2 . The Debye–Bueche plots produced a straight line for the three PU-PS IPN samples. Although increasing internetwork grafting in the PS component, the correlation length changed little.

Figure 4 shows the plots of $\tan \delta$ versus temperature for the three PU-PS IPN samples. It can be observed that the grafting agent strongly in-

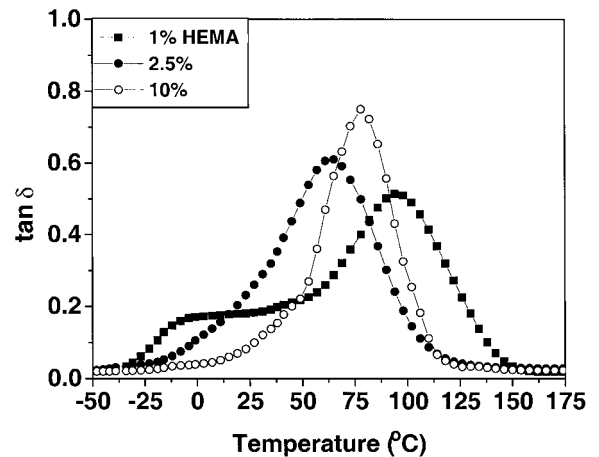


Figure 4 $\tan \delta$ versus temperature plots for the PU-PS (60 : 40 by weight) IPNs. (a) 1 wt % HEMA, (b) 2.5 wt % HEMA, and (c) 10 wt % HEMA.

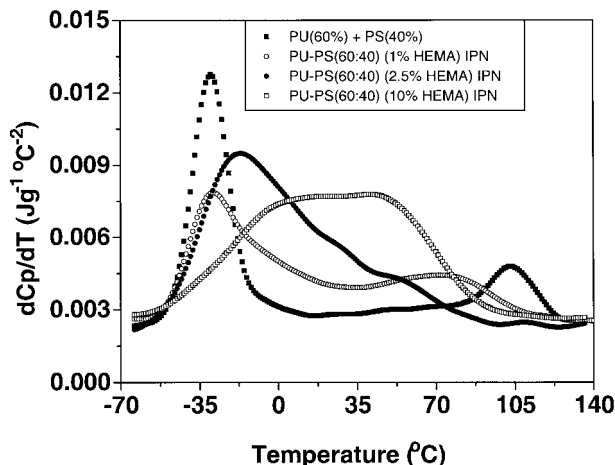


Figure 5 dC_p/dT versus temperature plots for the PU-PS (60 : 40) IPN with 1, 2.5, and 10 wt % HEMA and the PU network + PS network (60 : 40 by weight; physical blend), respectively.

fluenced the transition profile. Two distinct transition peaks in the $\tan \delta$ curve was found for the PU-PS IPN with 1 wt % HEMA. At an incorporation level of 2.5 wt % HEMA, one wide loss factor transition was observed. At 10 wt % HEMA, only one relatively narrow transition was found. The DMTA results showed that with increasing the internetwork grafting agent, the morphology of the PU-PS IPN became homogeneous.

Although the weight fraction of the PS component is 40%, the $\tan \delta$ peak for the PS component is much higher than that for PU component in the IPN with 1 wt % HEMA.

Recently, the application of the differential of heat capacity dC_p/dT versus temperature signal from M-TDSC to the characterization of the phase structure of IPNs has been developed.^{19,20} Here, dC_p/dT signal was again used to analyze the three PU-PS IPNs.

Figure 5 shows dC_p/dT versus temperature for the three PU-PS IPN samples and the PU networks + PS networks (60 : 40 by weight; physical blends) respectively. Comparing the dC_p/dT signals of the three PU-PS IPNs with their equivalent physical blends, it was observed that the dC_p/dT signal of the blend systems was quite different from that of their physical blends. Between their glass transition temperatures, the values of dC_p/dT signals of the IPN systems are larger than that of the physical blends. This indicates there is a transition in this temperature range. From these M-TDSC results, it can be concluded that the morpholo-

gies of the three PU-PS IPNs are multiphase structures, i.e., PU-rich and PS-rich phases plus interphases.

As shown earlier,^{19,20} for polymers and miscible polymer blends, the dC_p/dT versus temperature signal can be described by a Gaussian function G of temperature, the increment of heat capacity ΔC_p , the glass transition temperature T_g , and the half width of the glass transition peak (from dC_p/dT vs. temperature signal) ω_d .

$$G = \Delta C_p / [\omega_d (\pi/2)^{1/2}] \exp[-2(T - T_g)^2 / \omega_d^2] \quad (12)$$

Consider that there exist interphases in the three PU-PS IPNs. The dC_p/dT versus temperature signals for the PU-PS IPNs was divided by a peak resolution method^{9,20} into three parts that are related to PU-rich and PEMA-rich phases and interphases. The phase which has the lowest T_g is considered as PU-rich phase. The phase that has the highest T_g is considered as PS-rich phase. Other phases located between PU-rich and PS-rich phases are considered as interphases. Thus, the amount of interphases can be calculated.

Figure 6 shows the peak-resolution^{9,20} results for the PU-PS (60 : 40 by weight) IPN with 1 wt % HEMA. The baseline was subtracted based on the method suggested in Ref. 20. The weight fraction of interphases for the IPN was found to be 42%. Obviously, the degree of phase mixing (interphases) was quite high.

It has been reported^{7,8} that $\ln[I(s)s^4]$ versus s^2 plots had positive slopes for polyacrylate/epoxy

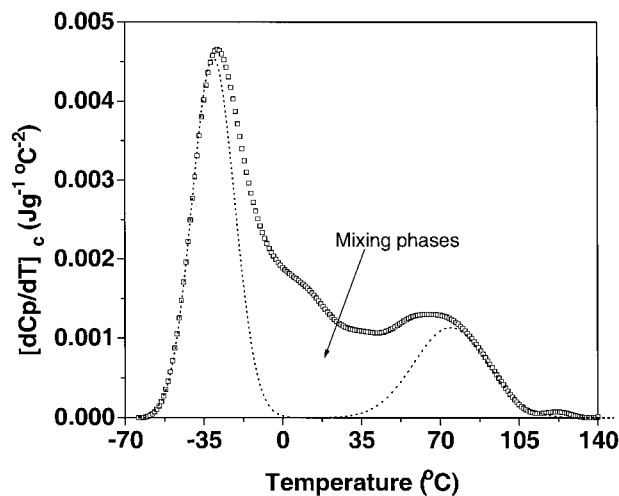


Figure 6 Interphases in the PU-PS (60 : 40) IPN with 1 wt % HEMA.

IPNs⁷ and for PU–poly(ethyl methacrylate) IPNs.⁸ According to Ruland's method mentioned above, the interfacial thickness cannot be conducted. M-TDSC and DMTA results indicated clearly there are interfacial diffuse boundaries in these IPNs. From M-TDSC and DMTA data, it is clear that the morphologies of these IPNs are complicated. For example, the morphology of PU-PS (60 : 40) with 1 wt % HEMA IPN consists of four kinds of networks, i.e., pure PU network, PU-rich network, PS-rich network, and interfacial network. The complicated morphology in these IPNs should result in complicated scattering behavior. Equation 2 may be invalid for the analysis in calculation of the interfacial thickness of these IPNs.

On other hand, the most important aspect of the analysis for the interfaces is its tremendous sensitivity to the subtraction of the thermal fluctuation scattering.²¹ Ruland et al.²² demonstrated in an investigation of styrene–isoprene triblock copolymer interfaces variations in interfacial thickness of $\pm 40\%$ when the fluctuation intensity used altered by only $\pm 2\%$. In order to overcome the weakness of this method in the subtraction of the thermal fluctuation scattering here, a new SAXS method was suggested to quantify the interfacial thickness.

The specific interfacial area S/V , defined as the ratio of interfacial surface area S to the volume V of phases is given by¹⁸

$$S/V = 4\phi(1 - \phi)/\alpha_c \quad (13)$$

The ϕ is the volume fraction of one of the phases. Equation (13) has been applied to IPNs.^{7,18} Equation 13 is independent of any morphological model.¹⁸

Define δ is the average interfacial thickness. Consider $\delta \ll V^{1/3}$. δS is equal to the volume of the interface. Assume that eq. (13) is still valid in this case. Then the volume fraction ω of the interface can be given by

$$\omega = \delta S/V \quad (14)$$

Combining eqs. (13) and (14), the interfacial thickness can be calculated by the following equation:

$$\delta = \omega\alpha_c/[4\phi(1 - \phi)] \quad (15)$$

This is the relationship between the interfacial thickness, the volume fraction of the interface and the correlation length. The volume fraction of interface can be determined by means of M-TDSC. The correlation length can be measured by using SAXS. Obviously, it is important to obtain an accurate value of the volume fraction of the interface in IPNs for the use of eq. (15). Quantification of the weight fraction of interphases in IPNs has been reported.^{19,20} However, it is not easy to quantify the volume fraction of the interface in IPNs. This will be main work in next paper.²³

Some differences between the M-TDSC and the DMTA data were in evidence. In addition to a difference in sensitivity to phase-separated structures, the observed transition magnitudes and the T_g shifts with increasing internetwork grafting also were different. The PU-rich transition was clearly dominant in the M-TDSC traces. M-TDSC measurements are more sensitive to a difference in heat capacity and weight fraction of polymers, whereas DMTA are more sensitive to the degree of phase continuity.

CONCLUSIONS

1. Both dCp/dT from M-TDSC and $\tan \delta$ from DMTA can be used to investigate the transition behavior of IPNs. The dCp/dT signal is much more sensitive to interphases. The dCp/dT data showed that the PU-PS (60 : 40 by weight) IPN with 10 wt % HEMA had a multiphase structure whereas the DMTA data showed that it was homogeneous.
2. SAXS data showed that with increasing internetwork grafting in the PS component, the domain size decreased. However, the correlation length was not sensitive to the internetwork grafting density in these IPNs.
3. According to the SAXS data, the determination of interfacial thickness for the three IPNs was unsuccessful. A new calculation method is needed.
4. M-TDSC and DMTA data showed that with increasing internetwork grafting density, the degree of phase mixing increased. Based on M-TDSC data, the weight fraction of interphases in IPNs can be quantified unlike the case with DMTA data.

REFERENCES

1. Klempner, D.; Sperling, L. H.; Utracki, L. A. American Chemical Society, Washington, DC, 1994.
2. Pandit, S. B.; Nadkarni, V. M. *Macromolecules* 1994, 27, 4583.
3. Russell, T. P.; Lee, D. S.; Nishi, T.; Kim, S. C. *Macromolecules* 1993, 26, 1922.
4. Shibayama, M.; Hashimoto, T. *Macromolecules* 1986, 19, 740.
5. Parizel, N.; Mayer, G.; Weill, G. *Polymer* 1995, 36, 2323.
6. Yang, J.; Winnik, M. K.; Ylitalo, D.; DeVoe, R. J. *Macromolecules* 1996, 29, 7055.
7. Tan, S.; Zhang, D.; Zhou, E. *Polymer* 1997, 38, 4571.
8. Song, M.; Hourston, H. J.; Schafer, F.-U. *Polymer* 1999, 40, 5773.
9. Ruland, R. *J. Appl Crystallogr* 1971, 4, 70.
10. Hourston, D. J.; Song, M.; Schafer, F. U.; Pollock, H. M.; Hammiche, A. *Polymer* 1999, 40, 4769.
11. Nevissas, V.; Widmaier, J. M.; Meyer, G. C. *J Appl Polym Sci* 1988, 36, 1467.
12. Hourston, D. J.; Zia, Y. *J Appl Polym Sci* 1984, 29, 629.
13. Scarito, P. R.; Sperling, L. H. *J Polym Sci* 1974, C46, 175.
14. Porod, G. *Kolloid Z* 1951, 124, 94.
15. Rathje, J.; Ruland, W. *Colloid Polym Sci* 1976, 254, 358.
16. Wiegand, W.; Ruland, W. *Prog Colloid Polym Sci* 1979, 66, 355.
17. Koberstein, J. T.; Morra, B.; Stein, R. S. *J Appl Cryst* 1980, 13, 34.
18. An, J. H.; Sperling, A. M. *Macromolecules* 1987, 20, 679.
19. Song, M.; Hourston, D. J.; Schafer, F. U.; Pollock, H. M.; Hammiche, A. *Thermochim Acta* 1998, 315, 25.
20. Song, M.; Hourston, D. J.; Reading, M.; Pollock, H. M.; Hammiche, A. *J Thermal Anal* 1999.
21. Foster, M. D. *Crit Rev Anal Chem* 1993, 24, 179.
22. Ruland, W. *Macromolecules* 1987, 20, 87.
23. Song, M. *J Appl Polym Sci*, submitted.